Maximization of Data Return at X-Band and Ka-Band on the DSN's 34-Meter Beam-Waveguide Antennas

S. Shambayati[1]

In this article, three new approaches to evaluating the performance advantage of the 32-GHz (Ka-band) frequency over the 8.4-GHz (X-band) frequency for receiving spacecraft downlink from deep-space missions are offered. For a given elevation profile for a pass, these approaches use atmospheric noise temperature statistics to select either the optimum data rate or the optimum data rate profile that maximizes the total data-return volume over the pass. For illustration purposes, these approaches are used to optimize the performance of a link for both X-band and Ka-band at Deep Space Network (DSN) 34-m beam-waveguide tracking stations at both Madrid, Spain, and Goldstone, California. Calculations show that by using these approaches an optimized Ka-band link, depending on the pass and the optimization method, offers between 4.7 dB and 7.2 dB more data volume than an optimized X-band link and between 7.0 dB and 10.9 dB more than an X-band link as currently operated by the DSN. These approaches provide performance gains in terms of average data return at the cost of reliability of the link or reduced tracking time or both. The reduced reliability of the link can have adverse effects in the continuity of the data returned, which in turn can make the link performance unacceptable.

I. Introduction

NASA's Deep Space Network (DSN) is in the process of making its 34-m beam-waveguide (BWG) antennas capable of receiving 32-GHz (Ka-band) signals. This is largely due to the fact that the 32-GHz frequency has the potential of offering as much as 11.6 dB more data than 8.4-GHz (X-band) for the same spacecraft antenna size, spacecraft antenna efficiency, and spacecraft transmitted power. This advantage is wholly attributable to the ground-system performance. However, since the Ka-band received signal-to-noise ratio (SNR) is more susceptible to large variations due to weather effects than is the X-band SNR and since Ka-band receiver electronics have a higher noise figure than do X-band receiver electronics, not all of this advantage is realizable.

---

[1] Communications Systems and Research Section.

The research described in this publication was carried out by the Jet Propulsion Laboratory, California Institute of Technology, under a contract with the National Aeronautics and Space Administration.

Previously, the analysis had focused on evaluating the advantage of Ka-band over X-band at fixed elevations (see [1] for example) or for a given link reliability (see [2]). However, as deep-space missions have expressed interest in Ka-band, a more comprehensive approach is needed to evaluate the performance advantage of Ka-band over a whole pass. This article presents three different approaches based on the statistical gain-to-temperature ratio, G/T, performance of the ground system over a pass. The first method selects a single data rate for the pass from 10-deg elevation to 10-deg elevation such that the average data volume returned over the pass is optimized. This approach is simple to implement and uses the whole tracking time. However, a link designed in such a manner is relatively unreliable. The second approach is similar to the first approach except that in order to improve the reliability of the link the spacecraft is tracked only when the reliability of the link for the selected data rate is above a given value. This approach again is simple to implement and improves the reliability of the link. However, this approach reduces the tracking time for the pass. The third approach uses a variable data rate (either continuously varying or varying in a stepwise fashion) to maximize the data return without significantly reducing the tracking time or the link reliability. However, this approach is complex and may be difficult to implement. Using these approaches, a Ka-band link offers between 4.74 dB and 7.2 dB more average data volume than an optimized X-band link and between 7.0 dB and 10.9 dB more than an X-band link designed according to current DSN practices.

The article is organized in the following manner: Section II introduces the mathematical foundations of this study and the optimization methodologies. Section III establishes the current DSN baseline performance by evaluating the performance of the X-band link at the 34-m BWG antennas under current DSN link design and operation practices for four typical passes. Section IV applies the single-data-rate optimization method to these passes for both X-band and Ka-band, and its performance is compared to the baseline performance established in Section III. Section V uses the modified single-data-rate algorithm to obtain optimized results. These results are again compared to the results in Section III. Section VI presents the results for the variable-data-rate optimization method. Conclusions are drawn and the limitations of the optimization approaches are outlined in Section VII.

II. Theoretical Foundation

A. Basic Equations

Consider a deep-space telecommunication link. Ignoring the power that is put in the carrier portion of the downlink signal, the instantaneous supportable data rate, R, is directly proportional to the ground antenna's gain-to-system noise temperature ratio, Γ, so that

$$R = \alpha \times \Gamma \tag{1}$$

where α is determined by a combination of the required bit signal-to-noise ratio, E_b/N_0, and the flux density received at the antenna. As α is a constant for the calculations in this article, it is assumed to be equal to 1. This assumption is equivalent to assuming that, for each frequency, the effective spacecraft antenna size and transmitted power are the same.

As the tracking elevation changes, Γ is affected by three parameters: the atmospheric noise temperature, T_{atm}, which also affects the path loss through the atmosphere and thus the effective gain of the antenna; the receiver and ground equipment noise temperature, T_{vac}; and the change in gain of the antenna, G, due to change in the deformation of the main antenna reflector. Mathematical models have been developed based on direct measurements that fully characterize G and T_{vac} as a function of the elevation for both X-band and Ka-band.[2] Therefore, the only unknown in evaluating Γ is T_{atm}.

[2] S. D. Slobin, "BWG Antenna Equations for Downlink Vacuum Gain and Vacuum Noise Temperature, Plus Values for Uplink Power and Gain, and Conscan Pointing Loss," JPL Interoffice Memorandum 3315-98-04 (internal document), Jet Propulsion Laboratory, Pasadena, California, January 30, 1998.

Since T_{atm} is a random variable, so is Γ. Complete probability distributions for T_{atm} at zenith are available based on actual measurements at both the Madrid and Goldstone Deep Space Communications Complexes (MDSCC and GDSCC, respectively) [1,3] at both X-band and Ka-band. Therefore, using these distributions along with the models for a 34-m BWG, probability distributions for Γ at each complex for these frequencies at any given elevation can be calculated. From this, $F(\gamma, \theta)$ is defined as

$$F(\gamma, \theta) = \Pr\{\Gamma > \gamma | \text{elevation} = \theta\} \tag{2}$$

This corresponds to the probability that a link designed with a required Γ of γ at elevation θ will successfully close. In other words, $F(\gamma, \theta)$ is the *instantaneous reliability* of a link designed for a Γ of γ at elevation θ. Given this, the instantaneous throughput for the link design with the required Γ of γ at elevation θ is given by

$$R_p(\gamma, \theta) = \gamma \times F(\gamma, \theta) \tag{3}$$

Conversely,

$$G(p, \theta) = \gamma \ni F(\gamma, \theta) = p \tag{4}$$

corresponds to the antenna Γ at elevation θ that is reliable a fraction of the time, p.

Given a data rate profile, $\gamma(t)$, and an elevation profile, $\theta(t)$, the average data volume returned over the pass is given by

$$V\big(\gamma(t)\big) = \int_{t_s}^{t_f} \gamma(t) \times F\big(\gamma(t), \theta(t)\big) \times dt \tag{5}$$

where t_s is the start time for the pass and t_f is the finish time. Furthermore, the average reliability of the pass is defined as the expected amount of time that the link closes during the pass over the pass duration and is given by

$$A\big(\gamma(t)\big) = \frac{1}{t_f - t_s} \int_{t_s}^{t_f} F\big(\gamma(t), \theta(t)\big) \times dt \tag{6}$$

B. Standard Link Design

In this subsection, the methodology for calculating the data return for a link designed according to standard DSN practices is presented. The standard DSN link is designed with a single data rate that closes for 90 percent weather (i.e., the link is reliable 90 percent of the time) at a 10-deg elevation (the nominal minimum tracking elevation used by the DSN) with 3 dB of margin, and the spacecraft is tracked from 10-deg elevation to 10-deg elevation. This 3 dB of margin is used to keep the link robust in the presence of unforeseen degradations in the link signal-to-noise ratio, such as degradations due to weather or antenna mispointing. Therefore, for the standard link, the design γ, γ_{std}, is defined as

$$\gamma_{std} = 0.5 \times G\left(0.9, 10^{\circ}\right) \tag{7}$$

Applying this to Eqs. (5) and (6), the standard average data-return volume is defined as

$$V_{std} = \int_{t_s}^{t_f} \gamma_{std} \times F\big(\gamma_{std}, \theta(t)\big) \times dt \tag{8}$$

and the standard average reliability is defined as

$$A_{std} = \frac{1}{t_f - t_s} \int_{t_s}^{t_f} F\big(\gamma_{std}, \theta(t)\big) \times dt \tag{9}$$

C. Single-Data-Rate Optimization (SRO)

In this subsection, a methodology is presented by which a single data rate that maximizes the average data return over the whole pass can be selected. The spacecraft is still tracked from 10-deg elevation to 10-deg elevation. This is similar to the standard link design except that the design data rate is optimized to return the maximum average data volume. In other words, the design data rate is γ_{opt}, such that

$$V(\gamma_{opt}) \geq V(\gamma) \ \forall \ \gamma \tag{10}$$

Based on this, the average reliability of the pass is given by $A\left(\gamma_{opt}\right)$. Note that while this approach increases the average data return, it reduces, at times, the instantaneous reliability of the link and the average reliability of the link overall.

D. Modified Single-Data-Rate Optimization (MSRO)

The approach outlined above is a single-data-rate approach and may cause the link to be highly unreliable at times during the pass. Therefore, two other approaches are considered for optimizing the link performance. The first involves limiting the pass to the time when the reliability of the link is above a certain level, p. The other involves varying the data rate with the elevation so that the link will have uniform reliability throughout the track.

For the first case, the indicator function, $I_p(x)$, is defined as

$$I_p(x) = \begin{cases} 1 & x \geq p \\ 0 & \text{otherwise} \end{cases} \tag{11}$$

Now, assuming that the link is designed so that it closes with a Γ of γ and has a required reliability of p so that the spacecraft is tracked only for that portion of the pass that the reliability is above p, the average data volume over the pass will be given by

$$\begin{aligned} V_p(\gamma) &= \int_{t_s}^{t_f} R_p\big(\gamma, \theta(t)\big) \times I_p\left(F\big(\gamma, \theta(t)\big)\right) \times dt \\ &= \int_{t_s}^{t_f} \gamma \times F\big(\gamma, \theta(t)\big) \times I_p\left(F\big(\gamma, \theta(t)\big)\right) \times dt \end{aligned} \tag{12}$$

A new optimum value for γ, $\gamma_{opt}^{(p)}$, is defined under this mode of tracking as

$$V_p\left(\gamma_{opt}^{(p)}\right) \geq V_p(\gamma) \ \forall \ \gamma \tag{13}$$

Furthermore, the definition of average reliability of the pass is modified to

$$A_p(\gamma) = \frac{\int_{t_s}^{t_f} F\big(\gamma, \theta(t)\big) \times I_p\left(F\big(\gamma, \theta(t)\big)\right) \times dt}{\int_{t_s}^{t_f} I_p\left(F\big(\gamma, \theta(t)\big)\right) \times dt} \tag{14}$$

Note that under this mode of tracking the actual start and finish times for the track are different from t_s and t_f, respectively, and depend on γ and p. Furthermore, since the actual tracking time under this type of tracking is less than $t_f - t_s$, then

$$V(\gamma_{opt}) \geq V_p\left(\gamma_{opt}^{(p)}\right) \tag{15}$$

Therefore, by using this type of tracking, data volume and tracking time are lost in order to gain reliability.

E. Variable-Data-Rate Tracking

As mentioned above, another way of increasing the reliability of the link is to use a variable data rate. There are two ways of modeling this. The first is to use a continuously variable data rate (CVDR). The other is to use a stepwise variable data rate (SVDR).

For the CVDR case, the average data returned over the pass is given by

$$V_{\mathrm{CVDR}}(p) = \int_{t_s}^{t_f} p \times G\big(p, \theta\,(t)\,\big) \times dt \tag{16}$$

In this case, by definition the reliability of the link is p. Furthermore, the optimization is performed with respect to p. Therefore, $p_{opt}^{(\mathrm{CVDR})}$ is defined as

$$V_{\mathrm{CVDR}}\left(p_{opt}^{(\mathrm{CVDR})}\right) \geq V_{\mathrm{CVDR}}(p) \;\; \forall \;\; p \tag{17}$$

Usually, the spacecraft transponder cannot continuously vary its data rate to follow $G\,(p, \theta\,(t))$. Therefore, under the SVDR case, $G\,(p, \theta\,(t))$ is approximated by a stepwise function that is always less than or equal to it. For SVDR tracking, the size of the step that can be taken depends on the spacecraft transponder capabilities and/or the ground system tracking limitations. Therefore, there are no set ways of evaluating the optimum data return under SVDR tracking. However, one approach that can be taken is to follow $G\,(p, \theta\,(t))$ with fixed-size (in dB) steps. Let η be the size of the step in dB; then define the function $G_s\,(p, \eta, t)$ as

$$G_s\,(p, \eta, t) = G\big(p, \theta(t_s)\big) \times 10^{(\eta/10) \times \lfloor 10 \log[G(p,\theta(t))] - 10 \log[G(p,\theta(t_s))] / \eta \rfloor} \tag{18}$$

where $\lfloor x \rfloor$ means the largest whole number greater than or equal to x.

Having defined $G_s\,(p, \eta, t)$, based on Eq. (5) the average data volume returned by the link is

$$V_{\mathrm{SVDR}}(p, \eta) = \int_{t_s}^{t_f} G_s(p, \eta, t) \times F\big(G_s(p, \eta, t), \theta(t)\big) \times dt \tag{19}$$

Furthermore, for a given η, the optimum value for p is defined as

$$p_{opt}^{(\mathrm{SVDR})}(\eta) \ni V_{\mathrm{SVDR}}\left(p_{opt}^{(\mathrm{SVDR})}(\eta), \eta\right) \geq V_{\mathrm{SVDR}}(p, \eta) \ \forall \ p \tag{20}$$

Finally, according to Eq. (6) the average reliability of the link is

$$A_{\mathrm{SVDR}}(p, \eta) = \frac{1}{t_f - t_s} \int_{t_s}^{t_f} F\big(G_s\left(p, \eta, t\right), \theta(t)\big) \times dt \tag{21}$$

Note that since $G_s\left(p, \eta, t\right)$ is always less than or equal to $G\big(p, \theta(t)\big)$, then $F\big(G_s(p, \eta, t), \theta(t)\big)$ is greater than or equal to p, and, thus, $A_{\mathrm{SVDR}}\left(p, \eta\right)$ is always greater than or equal to p.

The next four sections illustrate how these methods can be applied to evaluate the performance of both X-band and Ka-band links at a 34-m BWG station at both GDSCC and MDSCC.

III. Baseline Performance

In this article, four different elevation profiles are considered in order to evaluate the performance of the optimization methods presented. These profiles are shown in Fig. 1 and are taken from actual passes that tracked Mars Global Surveyor. These passes cover a wide range of maximum elevations so that the variations in the performance advantage of a Ka-band link over an X-band link can be understood. As a first step, the performances of the standard X-band link and standard Ka-band link, as they are currently used, are evaluated for these four elevation profiles.

As mentioned in Section II.B, the standard deep-space link is designed for a single data rate that closes the link at 10-deg elevation with a 3-dB margin for 90 percent weather. Looking at the tipping curves for the 34-m BWG antenna at X-band [Figs. 2(a and 2(b)], it is noted that for Goldstone an X-band link designed in such a manner closes with a γ of 49.8 dB and that for Madrid such a link closes with a γ of 49.5 dB. Looking at the same tipping curves, it is also noted that at 10-deg elevation these values

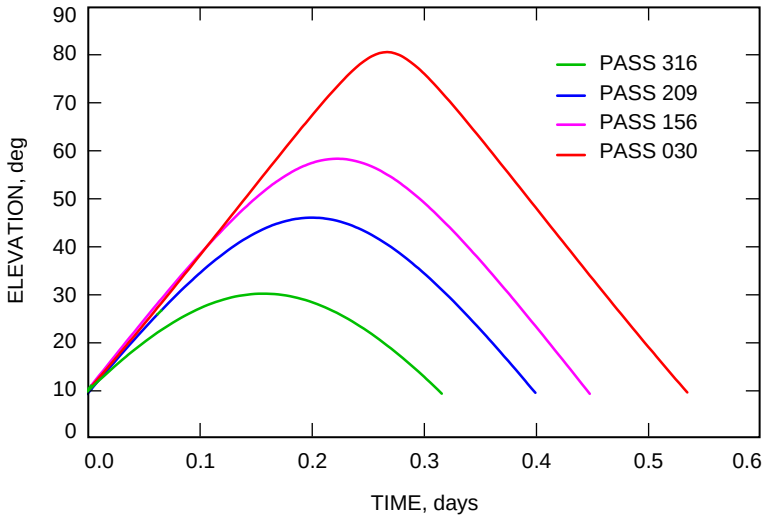

Fig. 1. Elevation versus time, passes 030, 156, 209, and 316.

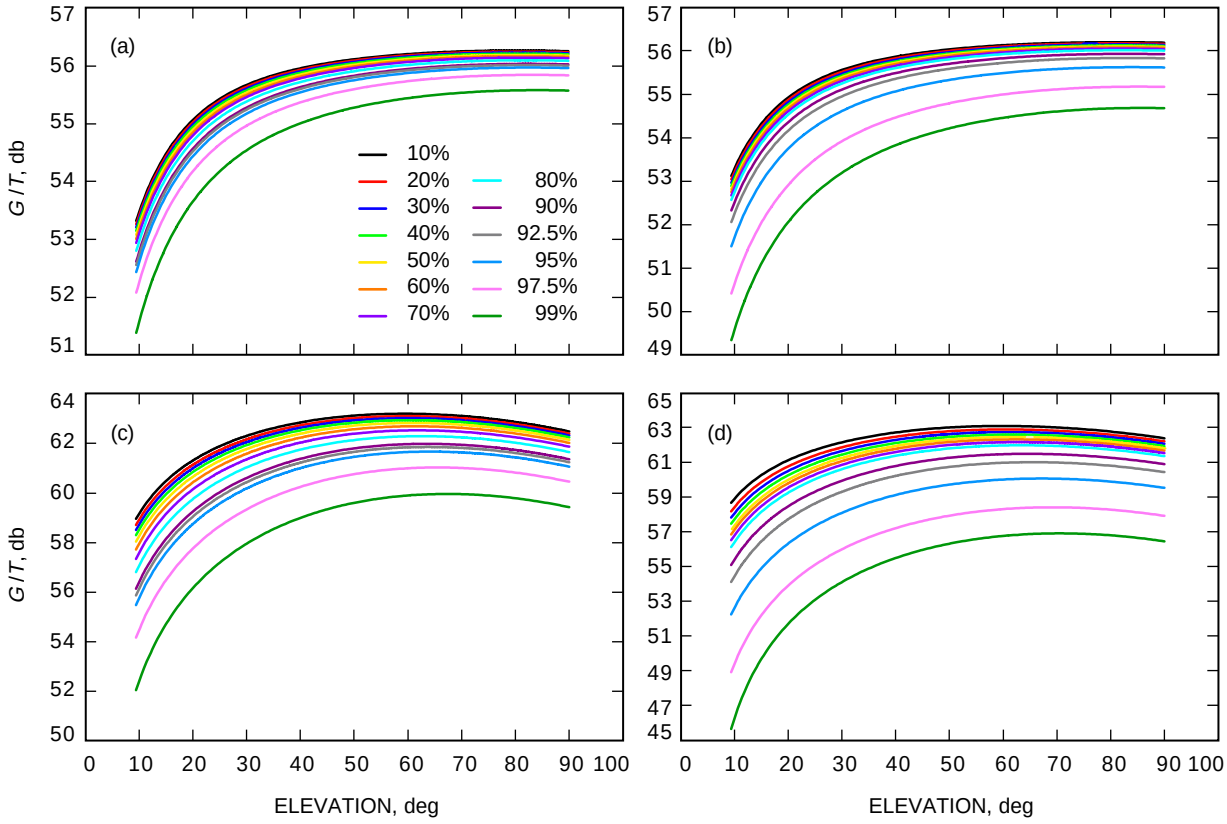

Fig. 2. Tipping curves for a 34-m BWG antenna: (a) X-band, Goldstone, (b) X-band, Madrid, (c) Ka-band, Goldstone, and (d) Ka-band, Madrid.

correspond to lower than 99 percent weather γ for Goldstone and between 97.5 and 99 percent weather γ for Madrid. Furthermore, as the elevation increases, both values become much less than 99 percent weather γ. This means that, through most of a typical pass, the reliability of a standard X-band link is better than 99 percent as far as the weather is concerned.

If the standard approach is applied to a Ka-band link, it is observed [Figs. 2(c) and 2(d)] that the link closes with a γ of 53.4 dB for Goldstone and 52.3 dB for Madrid. Looking at Figs. 2(c) and 2(d), it is also noted that, at 10-deg elevation, these values correspond to between 97.5 and 99 percent weather γ for Goldstone and between 95 and 97.5 percent weather γ for Madrid. This indicates that a Ka-band link designed in this fashion is less reliable than an X-band link.

Using the design γ values for the link at both X-band and Ka-band obtained through the standard approach, Eqs. (8) and (9) are applied to establish the baseline performances of both X-band and Ka-band for each pass. These results are presented in Tables 1 and 2. As seen from these tables, the standard X-band link is extremely reliable. The standard Ka-band link is also very reliable but not as reliable as the X-band link. Furthermore, the Ka-band data volume advantage is a constant 3.60 dB for Goldstone and an almost constant 2.78 dB for Madrid. These values roughly correspond to the difference between the design γ for Ka-band and the design γ for X-band. This is due to the fact that at each site the reliabilities of both X-band and Ka-band for all the passes are nearly 100 percent. Therefore, the difference in data volume between the two bands is equal to the difference between the design γ values.

Obviously, compared to the potential 11.6-dB performance advantage that Ka-band can offer over X-band, an advantage of 2.78 dB to 3.60 dB is disappointing. This is due to the fact that the standard

approach is too conservative and sacrifices performance for reliability. The next three sections will show that, by using the optimization methods outlined in the previous section, this advantage can be increased by as much as 7 dB.

Table 1. Ka-band and X-band average data return, standard link design, 34-m BWG antenna, Goldstone.

Pass	Ka-band, dB	X-band, dB	Ka-band advantage, dB	Ka-band average reliability, percent	X-band average reliability, percent
030	50.61	47.01	3.60	>99	>99
156	49.83	46.23	3.60	>99	>99
209	49.33	45.73	3.60	>99	>99
316	48.30	44.70	3.60	99	>99

Table 2. Ka-band and X-band average data return, standard link design, 34-m BWG antenna, Madrid.

Pass	Ka-band, dB	X-band, dB	Ka-band advantage, dB	Ka-band average reliability, percent	X-band average reliability, percent
030	49.50	46.71	2.79	98.7	>99
156	48.72	45.93	2.79	98.7	>99
209	48.22	45.43	2.79	98.6	>99
316	47.18	44.40	2.78	98.4	>99

IV. Single-Data-Rate Optimized X-Band and Ka-Band Links

In the previous section, it was shown that the standard link design does not fully utilize, in terms of average data volume, the capabilities of the Ka-band link. In this section, the methodology developed in Section II.C is used to show how the Ka-band link can be better utilized.

The optimum values of γ for both X-band and Ka-band were obtained for both Goldstone and Madrid for each pass. The optimum Ka-band average data return was then compared to both the standard X-band link average data return and the optimized X-band link average data return. The results of this analysis are presented in Tables 3 through 6.

As seen from these tables, for Goldstone, γ_{opt} for the Ka-band link is between 6.5 dB and 8 dB higher than the γ obtained by the standard link design approach. For Madrid, γ_{opt} is greater than the standard design γ by between 7.1 dB and 8.9 dB. For X-band, γ_{opt} is greater than the standard design γ by between 3 dB and 3.7 dB at Goldstone and between 3.1 dB and 3.9 dB at Madrid. It is also noted that the link's average reliability is much less under the SRO approach than it is under the standard link design approach. For the same elevation profile, the optimized link is less reliable at Madrid than it is at Goldstone. This is due to the fact that Madrid has worse weather than does Goldstone. The weather is subject to greater variations, thus making the Ka-band link less reliable.

In return for this decrease in average reliability, the average data return is increased over the standard link. For Ka-band, this increase is between 5.2 dB and 6.7 dB for Goldstone and between 5.7 dB and 7.2 dB for Madrid. For X-band, the increase in average data return is less. For Goldstone, this increase is between 2.5 dB and 3 dB, and for Madrid, this increase is between 2.5 dB and 3.1 dB. This indicates that a single-rate optimized Ka-band link not only has an advantage over the standard X-band link in terms of average data return (between 8.5 dB and 10.3 dB), but it also is approximately 4 to 5 times (6 dB to 7 dB) better than a single-rate optimized X-band link.

Table 3. Goldstone and Madrid γ_{opt} for X-band and Ka-band, SRO.

Pass	Goldstone		Madrid	
	Ka-band γ_{opt}, dB	X-band γ_{opt}, dB	Ka-band γ_{opt}, dB	X-band γ_{opt}, dB
030	61.4	53.5	61.2	53.4
156	61.2	53.4	60.9	53.3
209	60.8	53.3	60.5	53.1
316	59.9	52.8	59.4	52.6

Table 4. SRO average reliability of the link for X-band and Ka-band at Goldstone and Madrid.

Pass	Goldstone		Madrid	
	Average Ka-band reliability, percent	Average X-band reliability, percent	Average Ka-band reliability, percent	Average X-band reliability, percent
030	72.68	85.42	66.93	83.83
156	72.35	85.68	67.94	83.77
209	72.86	84.57	67.98	84.28
316	74.60	88.68	71.70	87.66

Table 5. SRO optimum average data return for Ka-band and X-band, and SRO optimum Ka-band advantage over SRO optimum X-band and standard X-band: Goldstone.

Pass	Optimum Ka-band, dB	Optimum X-band, dB	Ka-band advantage over optimum X-band, dB	Ka-band advantage over standard X-band, dB
030	57.27	50.07	7.20	10.26
156	56.27	49.21	7.07	10.04
209	55.40	48.55	6.85	9.67
316	53.58	47.23	6.35	8.88

Table 6. SRO optimum average data return for Ka-band and X-band, and SRO optimum Ka-band advantage over SRO optimum X-band and standard X-band: Madrid.

Pass	Optimum Ka-band, dB	Optimum X-band, dB	Ka-band advantage over optimum X-band, dB	Ka-band advantage over standard X-band, dB
030	56.71	49.89	6.82	10.00
156	55.70	49.01	6.69	9.77
209	54.80	48.33	6.47	9.37
316	52.90	46.98	5.93	8.50

V. Modified Single-Data-Rate Optimized X-Band and Ka-Band Links

As mentioned above, in exchange for the increase in the average data return, the average reliability of the link is substantially decreased for Ka-band. However, by looking at how the reliability of a pass changes as the elevation changes, it is noted that this decrease in reliability is not as serious as one might think. Figures 3(a) and 3(b) show plots of $F(\gamma_{opt}, \theta(t))$ (defined by Eq. (2) above) versus time for the four passes for Goldstone and Madrid, respectively. As these plots indicate, the reliability of an optimized Ka-band link increases as the elevation increases, and during each pass there is a substantial period of time when the link reliability is 90 percent or better. Since, statistically, most of the data returned are received during these high-reliability periods associated with higher elevations, the link can be operated only at these periods without too much loss of data. Therefore, the Ka-band advantage can still be realized without too much decrease in the reliability of the link. Under such a scenario, instead

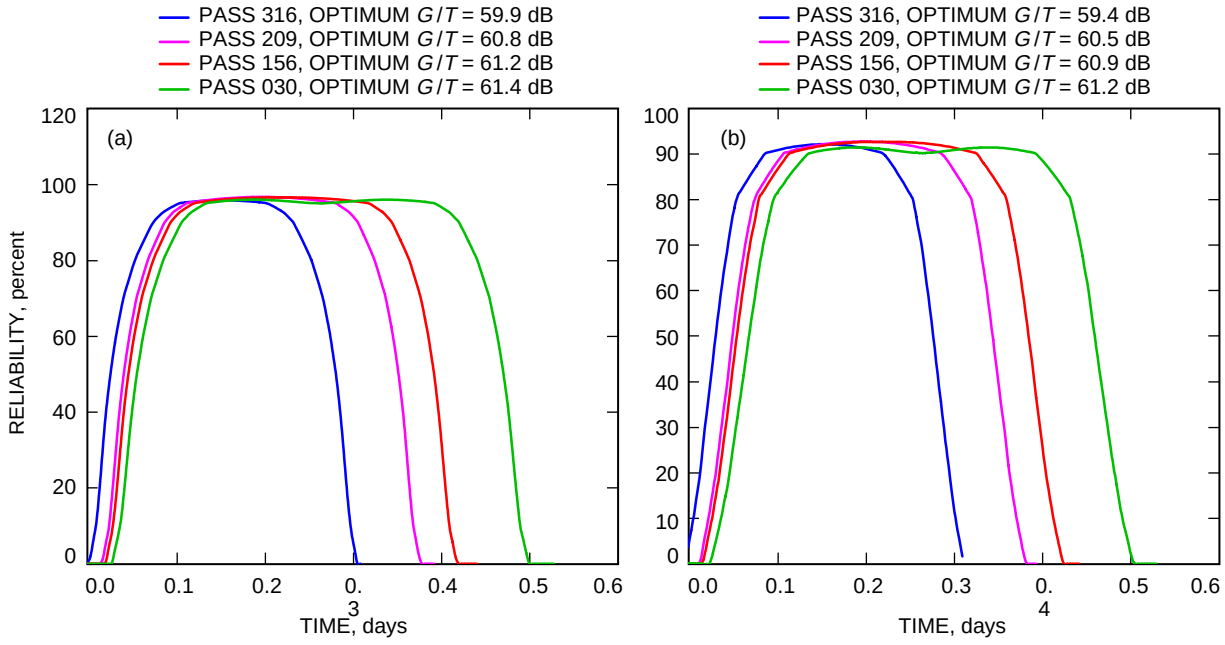

Fig. 3. Ka-band reliability versus time for a 34-m BWG antenna: (a) Goldstone and (b) Madrid.

of starting a pass at 10-deg elevation, the pass starts at a higher elevation depending on instantaneous reliability requirements. Using this approach, the values of $\gamma_{opt}^{(p)}$ for $p = 0.9$ were obtained, and the average total data return for each pass was evaluated for both X-band and Ka-band at Madrid and Goldstone. The results are shown in Tables 7 through 13 and Figs. 4(a) and 4(b).

As expected, these tables indicate that the total average data returned on an MSRO link is less than the average data returned on a comparable SRO link. However, the MSRO link is more reliable (see Table 9) and still provides a significant improvement in the average amount of data returned over the standard X-band link. The cost of this increased reliability of the link is between 0.9 dB (for pass 030 at Goldstone) and 1.5 dB (for pass 316 at Madrid) in terms of data return. In addition, MSRO uses between 66 and 75 percent of the tracking time of a pass (see Tables 12 and 13). This can be both good and bad. The reduced tracking time means that more spacecraft can be tracked than with SRO without too much loss of data from any particular mission. It also means that the missions will not have as much non-telemetry data (e.g., radio science and ranging) as they normally would have.

Table 7. Goldstone and Madrid $\gamma_{opt}^{(0.9)}$ for X-band and Ka-band, MSRO, $p = 0.9$.

Pass	Goldstone		Madrid	
	Ka-band $\gamma_{opt}^{(0.9)}$, dB	X-band $\gamma_{opt}^{(0.9)}$, dB	Ka-band $\gamma_{opt}^{(0.9)}$, dB	X-band $\gamma_{opt}^{(0.9)}$, dB
030	61.0	53.3	60.3	53.2
156	60.5	53.2	59.7	53.2
209	60.2	53.1	59.6	52.9
316	58.8	52.7	58.2	52.4

Table 8. MSRO pass minimum elevation for X-band and Ka-band at Goldstone and Madrid, $p = 0.9$.

Pass	Goldstone		Madrid	
	Ka-band minimum elevation, deg	X-band minimum elevation, deg	Ka-band minimum elevation, deg	X-band minimum elevation, deg
030	34.81	20.20	34.06	20.90
156	29.25	19.00	28.26	20.90
209	26.60	17.93	27.45	17.63
316	17.91	14.52	18.95	13.81

Table 9. MSRO average reliability of the link for X-band and Ka-band at Goldstone and Madrid, $p = 0.9$.

Pass	Goldstone		Madrid	
	Average Ka-band reliability, percent	Average X-band reliability, percent	Average Ka-band reliability, percent	Average X-band reliability, percent
030	96.37	98.67	93.44	97.65
156	96.93	98.62	94.13	97.25
209	96.61	98.59	93.43	97.33
316	96.72	98.45	93.41	96.86

Table 10. MSRO optimum average data return for Ka-band and X-band, and MSRO optimum Ka-band advantage over MSRO optimum X-band and standard X-band, $p = 0.9$: Goldstone.

Pass	Optimum Ka-band, dB	Optimum X-band, dB	Ka-band advantage over optimum, X-band, dB	Ka-band advantage over standard, X-band, dB
030	56.37	49.85	6.52	9.36
156	55.31	49.00	6.31	9.08
209	54.38	48.31	6.07	8.65
316	52.39	46.96	5.43	7.69

Table 11. MSRO optimum average data return for Ka-band and X-band, and MSRO optimum Ka-band advantage over MSRO optimum X-band and standard X-band, $p = 0.9$: Madrid.

Pass	Optimum Ka-band, dB	Optimum X-band, dB	Ka-band advantage over optimum, X-band, dB	Ka-band advantage over standard, X-band, dB
030	55.58	49.68	5.91	8.87
156	54.48	48.78	5.70	8.55
209	53.52	48.10	5.42	8.09
316	51.44	46.70	4.74	7.04

Table 12. MSRO Ka-band link pass duration, $p = 0.9$: Goldstone.

Pass	MSRO pass duration, days	Total pass duration, days	Fraction of total pass time used
030	0.354	0.528	0.671
156	0.309	0.441	0.701
209	0.267	0.392	0.681
316	0.233	0.309	0.753

Table 13. MSRO Ka-band link pass duration, $p = 0.9$: Madrid.

Pass	MSRO pass duration, days	Total pass duration, days	Fraction of total pass time used
030	0.358	0.528	0.678
156	0.316	0.441	0.717
209	0.260	0.392	0.664
316	0.222	0.309	0.719

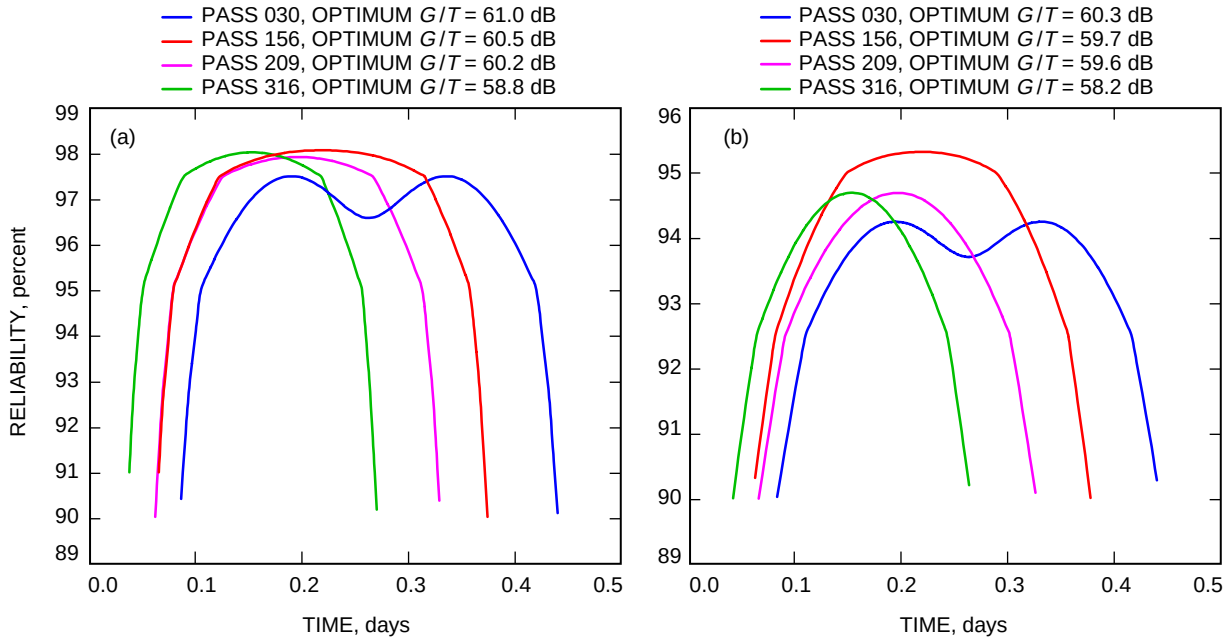

Fig. 4. MSRO Ka-band reliability versus time: (a) Goldstone and (b) Madrid.

VI. Continuously Variable Data-Rate and Stepwise Variable Data-Rate Optimization

In this section, the variable-data-rate optimization methods were applied to the four representative passes. The results of these optimizations are shown in Tables 14 through 18 and Figs. 5 through 8. As indicated by Tables 14 and 15, a Ka-band CVDR optimized link provides between 9.39 dB and 10.90 dB more data than the standard X-band link at Goldstone and between 9.15 dB and 10.70 dB more data at Madrid. Furthermore, as Figs. 5(a) and 5(b) indicate, the average data return for a Ka-band CVDR link changes very little between 70 and 95 percent weather for Goldstone (less 0.4 dB) and between 65 and 90 percent weather for Madrid (less than 0.6 dB). This means that by using CVDR the reliability of the link can be increased significantly without too much loss of data. Tables 14 and 15 also indicate that the optimized CVDR X-band link significantly outperforms the standard X-band link. Finally, Figs. 5(a) through 5(d) indicate that the X-band link pays less of a penalty in terms of average data return than does the Ka-band for increased reliability. Going from optimum weather to 99 percent weather for the Ka-band CVDR link costs between 1.9 dB (pass 030) and 2.4 dB (pass 316) of average data return at Goldstone and between 4.7 dB (pass 030) and 6.2 dB (pass 316) at Madrid. For the X-band CVDR link, going from optimum weather to 99 percent weather costs between 0.19 dB (pass 030) and 0.44 dB (pass 316) at Goldstone and between 1.2 dB (pass 030) and 1.8 dB (pass 316) at Madrid.

Table 14. Optimized average CVDR Ka-band and X-band data return, and CVDR optimized Ka-band advantage over CVDR optimized X-band and standard X-band: Goldstone.

Pass	Ka-band $P_{opt}^{(\mathrm{CVDR})}$, percent	Ka-band $V_{\mathrm{CVDR}}\left(P_{opt}^{(\mathrm{CVDR})}\right)$, dB	X-band $P_{opt}^{(\mathrm{CVDR})}$, percent	X-band $V_{\mathrm{CVDR}}\left(P_{opt}^{(\mathrm{CVDR})}\right)$, dB	Optimized Ka-band advantage over optimized X-band, dB	Optimized Ka-band advantage over standard X-band, dB
030	90	57.90	95	52.44	5.47	10.89
156	90	56.99	95	51.53	5.46	10.76
209	90	56.10	95	50.82	5.28	10.37
316	90	54.09	95	49.29	4.80	9.39

Table 15. Optimized average CVDR Ka-band and X-band data return, and CVDR optimized Ka-band advantage over CVDR optimized X-band and standard X-band: Madrid.

Pass	Ka-band $P_{opt}^{(\mathrm{CVDR})}$, percent	Ka-band $V_{\mathrm{CVDR}}\left(P_{opt}^{(\mathrm{CVDR})}\right)$, dB	X-band $P_{opt}^{(\mathrm{CVDR})}$, percent	X-band $V_{\mathrm{CVDR}}\left(P_{opt}^{(\mathrm{CVDR})}\right)$, dB	Optimized Ka-band advantage over optimized X-band, dB	Optimized Ka-band advantage over standard X-band, dB
030	80	57.38	90	52.15	5.23	10.67
156	80	56.46	90	51.24	5.22	10.53
209	80	55.58	90	50.53	5.05	10.15
316	80	53.56	90	48.99	4.58	9.16

Table 16. Optimized average 1-dB SVDR Ka-band and X-band data return, and 1-dB SVDR optimized Ka-band advantage over 1-dB SVDR optimized X-band and standard X-band: Goldstone.

Pass	Ka-band $P_{opt}^{(\mathrm{SVDR})}(1)$, percent	Ka-band $V_{\mathrm{SVDR}}\left(P_{opt}^{(\mathrm{SVDR})}(1)1\right)$, dB	X-band $P_{opt}^{(\mathrm{SVDR})}(1)$, percent	X-band $V_{\mathrm{SVDR}}\left(P_{opt}^{(\mathrm{SVDR})}(1)1\right)$, dB	Optimized Ka-band advantage over optimized X-band, dB	Optimized Ka-band advantage over standard X-band, dB
030	70	57.85	85	50.77	7.08	10.84
156	75	56.92	90	49.86	7.06	10.69
209	75	56.04	85	49.22	6.82	10.31
316	75	54.06	60	47.74	6.32	9.36

Table 17. Optimized average 1-dB SVDR Ka-band and X-band data return, and 1-dB SVDR optimized Ka-band advantage over 1-dB SVDR optimized X-band and standard X-band: Madrid.

Pass	Ka-band $P_{opt}^{(\mathrm{SVDR})}(1)$, percent	Ka-band $V_{\mathrm{SVDR}}\left(P_{opt}^{(\mathrm{SVDR})}(1)1\right)$, dB	X-band $P_{opt}^{(\mathrm{SVDR})}(1)$, percent	X-band $V_{\mathrm{SVDR}}\left(P_{opt}^{(\mathrm{SVDR})}(1)1\right)$, dB	Optimized Ka-band advantage over optimized X-band, dB	Optimized Ka-band advantage over standard X-band, dB
030	80	57.32	75	50.55	6.77	10.61
156	65	56.37	85	49.65	6.72	10.44
209	75	55.47	80	48.98	6.49	10.04
316	65	53.44	60	47.44	6.00	9.04

Table 18. Optimized 1-dB SVDR Ka-band and X-band pass average reliability: Goldstone and Madrid.

	Goldstone		Madrid	
Pass	Ka-band $A_{\mathrm{SVDR}}\left(P_{opt}^{(\mathrm{SVDR})}(1),1\right)$, percent	X-band $A_{\mathrm{SVDR}}\left(P_{opt}^{(\mathrm{SVDR})}(1),1\right)$, percent	Ka-band $A_{\mathrm{SVDR}}\left(P_{opt}^{(\mathrm{SVDR})}(1),1\right)$, percent	X-band $A_{\mathrm{SVDR}}\left(P_{opt}^{(\mathrm{SVDR})}(1),1\right)$, percent
030	86.39	97.15	85.39	93.22
156	88.90	97.25	83.80	93.93
209	88.33	96.72	83.85	92.70
316	86.46	94.77	80.86	92.00

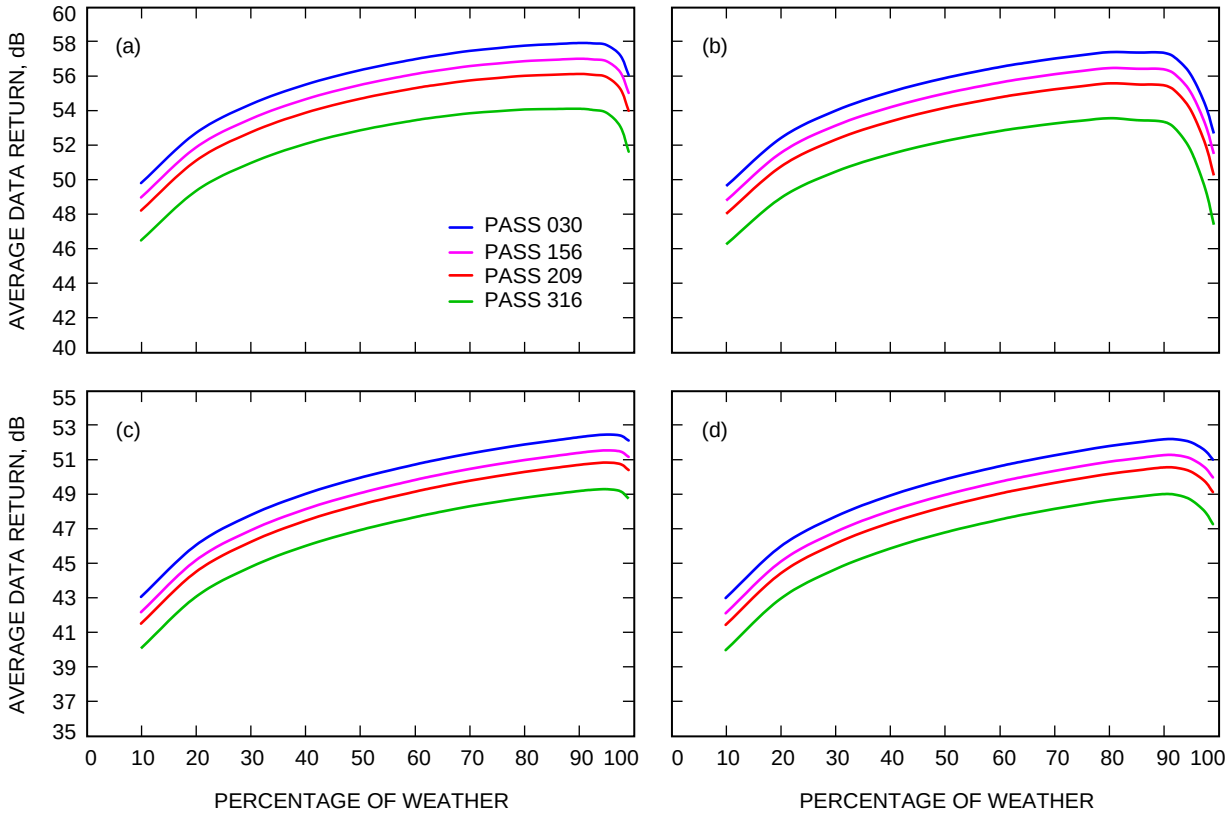

Fig. 5. Average CVDR data return versus percentage of weather: (a) Ka-band, Goldstone, (b) Ka-band, Madrid, (c) X-band, Goldstone, and (d) X-band, Madrid.

Tables 16 and 17 indicate that, while for Ka-band the optimized 1-dB SVDR provides almost as much gain over standard X-band for both Madrid and Goldstone as does the optimized CVDR link, the optimized 1-dB SVDR X-band link does not fully realize all the advantage of the optimized CVDR X-band link. This is due to the fact that there is little variation in Γ during the pass for the X-band link for any weather condition. Therefore, the 1-dB SVDR X-band data rate profile consists at most of two or three data rates. On the other hand, due to the large variation in the Ka-band Γ during the pass, the 1-dB SVDR goes through many data rate changes, thus closely following the Γ profile of the pass. Furthermore, Figs. 6(a) and 6(b) indicate that there is very little variation in total data return from 50 percent weather to 95 percent weather for Ka-band 1-dB SVDR at Goldstone (less than 0.6 dB) and from 50 percent weather to 90 percent weather for Madrid (less than 0.5 dB). This indicates that, by using 1-dB SVDR at higher percentage weather values, almost the same amount of data return can be achieved as with the lower weather percentages, with better reliability.

Figures 7(a) and 7(b) indicate the average reliability of the Ka-band link as a function of percentage of weather, and Figs. 7(c) and 7(d) indicate the same for X-band. As seen from these figures, the 1-dB SVDR average reliability is not necessarily an increasing function of percentage of weather. This is due to the fact that the 1-dB SVDR implementation under consideration is an arbitrary approximation of the Γ profile of the pass. Therefore, depending on the Γ profile of the pass at any particular moment, the reliability of the link can be either very close to p or very close to 100 percent. This is illustrated by Figs. 8 and 9. Figure 8 presents the X-band 1-dB SVDR Γ profile for 10 and 40 percent weather and the X-band Γ profile of 90 percent weather for pass 209 at Goldstone. As seen from this figure, a 10 percent weather 1-dB SVDR G/T profile is almost always less than a 90 percent weather Γ profile, while 40 percent weather is not. This means that the 10 percent 1-dB SVDR link has better average reliability than does the 40 percent 1-dB SVDR link. This indicates that, due to the arbitrary nature of

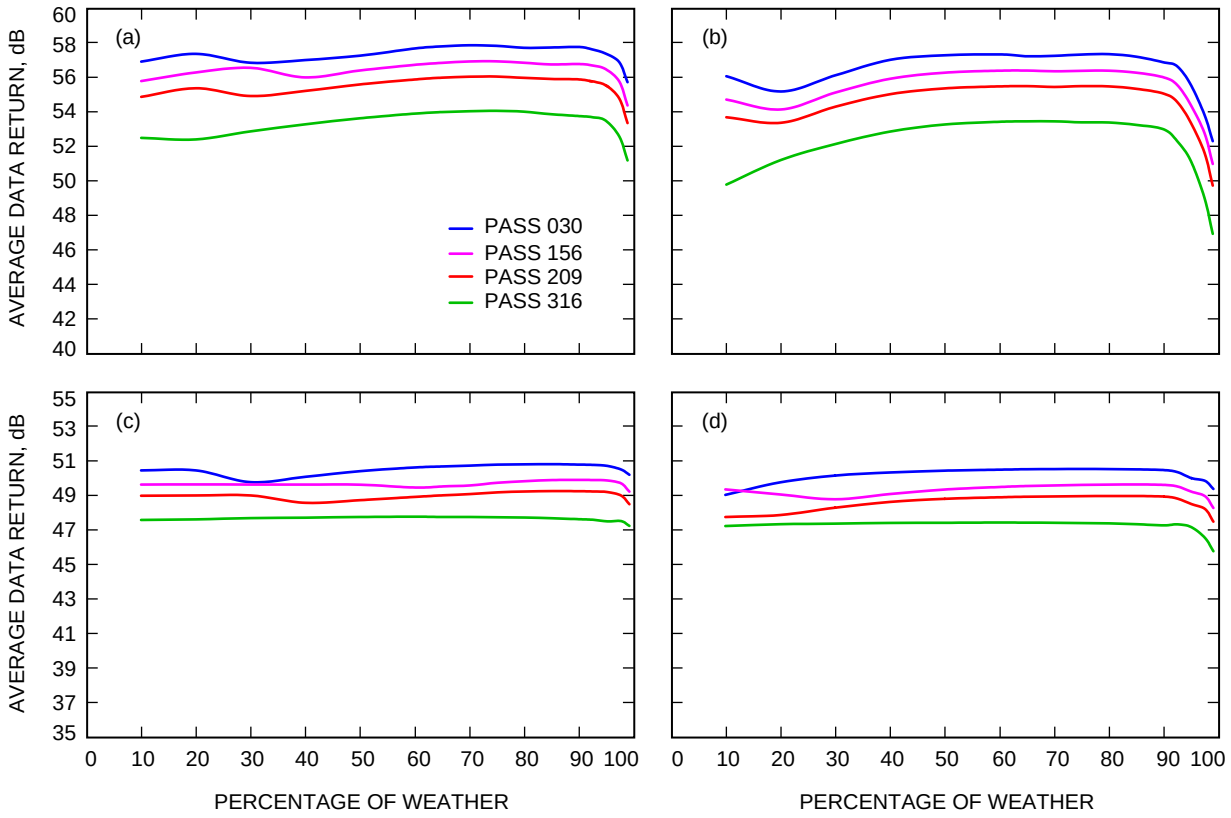

Fig. 6. 1-dB SVDR average data return versus percentage of weather: (a) Ka-band, Goldstone, (b) Ka-band, Madrid, (c) X-band, Goldstone, and (d) X-band, Madrid.

the 1-dB SVDR Γ profiles, $A_{\mathrm{SVDR}}\left(p_{opt}^{(\mathrm{SVDR})}(1), 1\right)$ can vary wildly. This also explains the non-monotonic nature of the 1-dB SVDR average data-return curves.

Finally, Figs. 7(a) through 7(d) again indicate that, in terms of average data volume, X-band pays less of a penalty for reliability than does Ka-band. The difference between optimum 1-dB SVDR data volume and 99 percent 1-dB SVDR data volume for Ka-band is between 2.1 dB (pass 030) and 2.9 dB (pass 316) at Goldstone and between 5 dB (pass 030) and 6.5 dB (pass 316) at Madrid. This same quantity for X-band is between 0.52 dB (pass 316) and 0.75 dB (pass 209) for Goldstone and between 1.16 dB (pass 030) and 1.71 dB (pass 316) for Madrid.

VII. Conclusions and Caveats

A. Conclusions

In this article, three different methods for optimizing the performance of a deep-space link were presented. The first two methods assume that a single data rate is used to transmit data during the pass and attempt to select the optimum data rate that maximizes the average amount of data returned over the pass. Under the first method (SRO), it is assumed that the tracking starts when the spacecraft is above 10-deg elevation in the sky and finishes when the spacecraft goes below 10-deg elevation. The second method (MSRO) assumes that the spacecraft is tracked only when the link has a reliability above a given level. The third method assumes that the data rate over the link can be varied to follow a given percentage of weather Γ profile either continuously or in a stepwise fashion. This method attempts to maximize the average data return by selecting the optimum percentage of weather Γ profile.

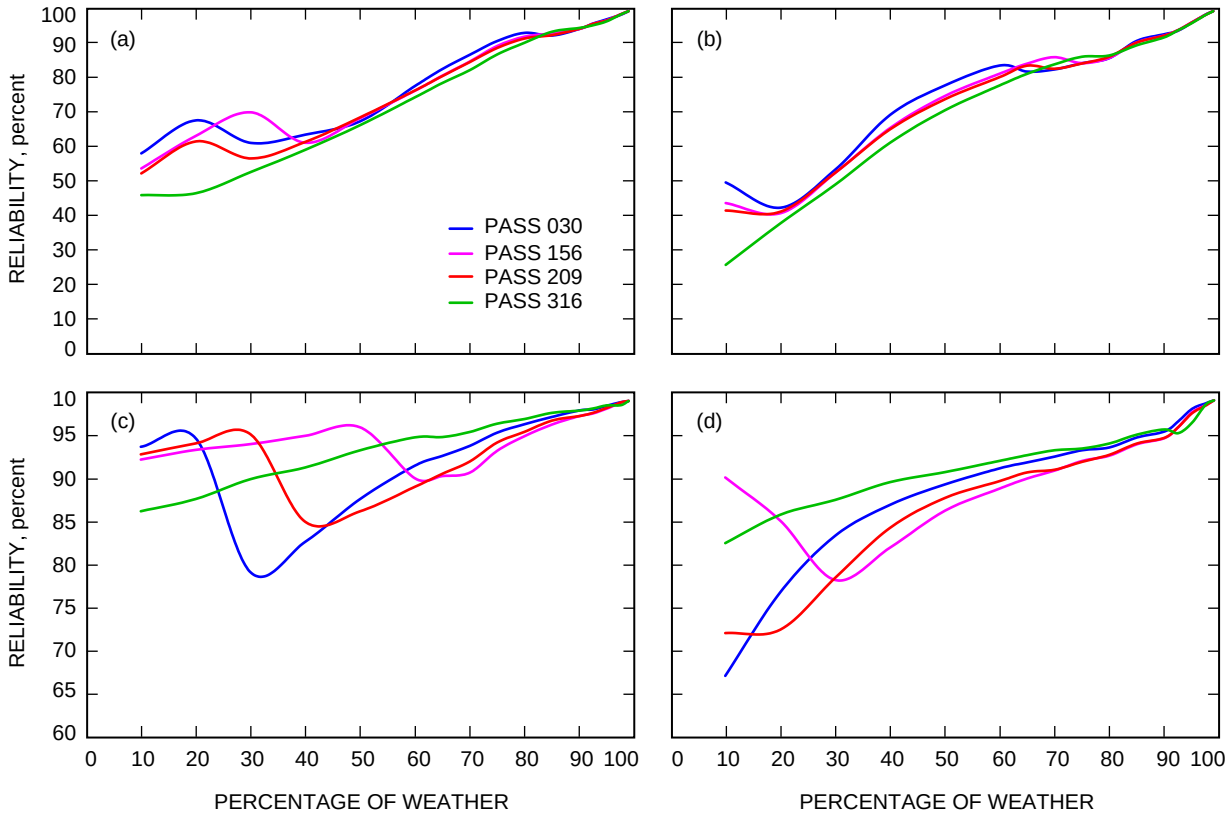

Fig. 7. 1-dB SVDR average pass reliability versus percentage of weather: (a) Ka-band, Goldstone, (b) Ka-band, Madrid, (c) X-band, Goldstone, and (d) X-band, Madrid.

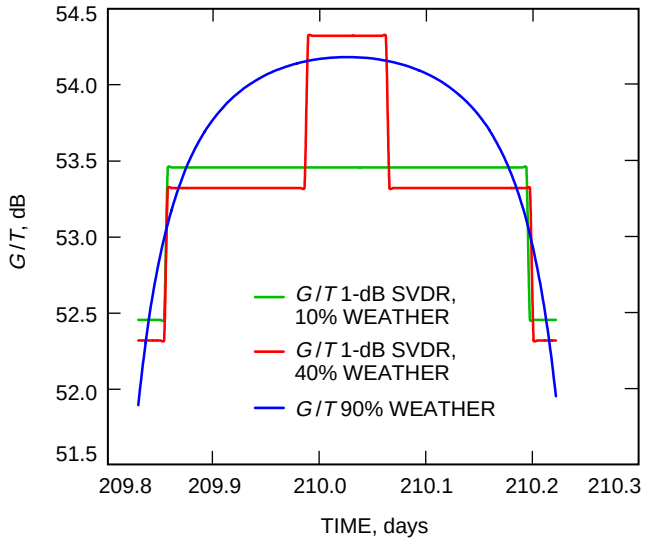

Fig. 8. X-band 1-dB SVDR *G*/*T* profile for 10 and 40 percent weather, and X-band *G*/*T* profile for 90 percent weather, for pass 209 at Goldstone.

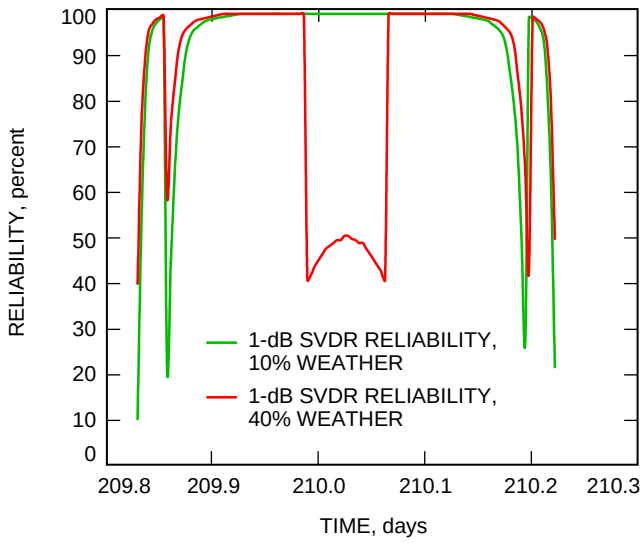

Fig. 9. X-band 1-dB SVDR 10 percent weather and 40 percent weather reliability versus time.

These methods were applied to four typical passes for X-band and Ka-band for 34-m BWG antennas at both the Goldstone and the Madrid Deep Space Communication Complexes, and the results were compared with the standard X-band link as currently designed by the DSN and with each other. In order to establish a baseline, the performance of the standard Ka-band link was also established. The standard Ka-band link has an advantage of only between 2.8 dB and 3.6 dB over the standard X-band link. The SRO Ka-band link provides between 8.5-dB and 10.3-dB better performance than the standard X-band link and between 5.9-dB and 7.2-dB better performance than the SRO X-band link. The MSRO Ka-band link with a minimum reliability of 0.9 provides between 7.0-dB and 9.4-dB better performance than the standard X-band link and between 4.5-dB and 6.5-dB better performance than the MSRO X-band link. For the variable-data-rate optimization, if a continuous data rate model is used, the optimum Ka-band link provides between 9.2-dB and 9.4-dB better performance than the standard X-band link and between 4.6-dB and 5.5-dB better performance than a similarly optimized X-band link. If a particular 1-dB stepwise variable-data-rate model is used, the optimum Ka-band link provides between 9.0-dB and 9.4-dB better performance than the standard X-band link and between 6.0-dB and 7.1-dB better performance than a similarly optimized X-band link.

These results also indicate that the reliability of the standard X-band link is almost 100 percent and the reliability of the standard Ka-band link is greater than 98.0 percent. The SRO Ka-band link is significantly less reliable, with its average reliability varying between 66.9 and 72.0 percent at Madrid and between 72.0 and 75.0 percent at Goldstone. The SRO X-band link has an average reliability of 83.0 to 88.0 percent at Madrid and 84.0 to 89.0 percent at Goldstone. The MSRO link achieves better reliability at the cost of reduced tracking time and reduced data return as compared with the SRO link. The 90 percent MSRO Ka-band link has a minimum average reliability of 93.0 percent at Madrid and 96.0 percent at Goldstone. The tracking time for the Ka-band 90 percent MSRO link is between 67.0 and 75.0 percent of the total tracking time for the other methods. For the 90 percent MSRO X-band link, the minimum average reliability is better than 96.5 percent at Madrid and better than 98.0 percent at Goldstone. For the continuous data rate optimization, the reliability of the Ka-band link is 90.0 percent for all passes at Goldstone and 80.0 percent for all passes at Madrid. However, for both these cases, the reliability can be increased significantly (10 percent for Madrid and 5 percent for Goldstone) without too much loss of data.

Of these methods, SRO and MSRO are equally simple to implement on the spacecraft and require no departure from current practices. SVDR requires complex sequencing of the spacecraft so the data

rate can be changed incrementally. CVDR requires a new type of spacecraft transponder that can vary its data rate continuously. On the ground side, SRO requires no departure from current practices, and MSRO requires a minor modification in calculation of the visibility window of the spacecraft at each site. CVDR and SVDR, on the other hand, require significant modifications of the ground tracking procedures and equipment, from creating predicts to modifying the ground receivers to accommodate changes in the data rate.

B. Caveats

It should be noted that one reason the standard X-band link does not offer as much data return as either of the optimized links (both X-band and Ka-band) for any of the optimization methods is that, in standard link design, 3 dB of margin at 10-deg elevation is allocated to keep the link robust and reliable. This 3 dB guards not only against adverse variations in the weather but also against such things as antenna mispointing and ground equipment malfunction. The optimization methods presented here do not take into account such variations.

Furthermore, throughout this article it has been assumed that the spacecraft power, spacecraft antenna size, and spacecraft antenna efficiency are the same for both X-band and Ka-band. Therefore, all the analysis presented here is the result of the Ka-band ground-system advantage over X-band. However, currently Ka-band amplifiers are less powerful and less efficient than X-band amplifiers, and, due to the narrower antenna beam at Ka-band, the spacecraft antenna pointing losses are greater at Ka-band than they are at X-band. All these factors cut into the Ka-band advantage that is reported in this article.

Finally, in all cases, these optimization methods increase the average data return at the expense of reliability of the link. While not always stated, most links have a requirement for continuity in the data. Because none of the optimized links is very reliable, they may have a hard time meeting most data continuity conditions. Such continuity conditions may require implementation of complex retransmission algorithms that can add to the complexity and difficulty of operations for the link.

References

[1] S. Shambayati, "Optimization of a Deep-Space Ka-band Link Using Atmospheric-Noise-Temperature Statistics," *The Telecommunications and Mission Operations Progress Report 42-139, July–September 1999*, Jet Propulsion Laboratory, Pasadena, California, pp. 1–16, November 15, 1999. http://tmo.jpl.nasa.gov/tmo/progress_report/42-139/139C.pdf

[2] M. A. Koerner, "Relative Performance of 8.5-GHz and 32-GHz Telemetry Links on the Basis of Total Data Return per Pass," *The Telecommunications and Data Acquisition Progress Report 42-87, July–September 1986*, Jet Propulsion Laboratory, Pasadena, California, pp. 65–80, November 15, 1986. http://tmo.jpl.nasa.gov/tmo/progress_report/42-87/87H.PDF

[3] *DSMS Telecommunications Link Design Handbook*, 810-005, Rev. E, Jet Propulsion Laboratory, Pasadena, California, November 30, 2000.